

# Dependency of parameter estimates for the tofts model on temporal sampling rate and on bolus arrival time

H. O. Laue<sup>1</sup>, M. Althaus<sup>1</sup>, S. Behrens<sup>1</sup>, H. K. Hahn<sup>1</sup>, and H-O. Peitgen<sup>1</sup>  
<sup>1</sup>Mevis Research, Bremen, Germany

**Introduction:** In recent years, there has been a trend toward applying a dedicated tracer kinetics model to contrast-enhanced MRI data in order to extract parameters reflecting the state of physiological tissue properties. A number of different models have been proposed in literature [1]. The temporal sampling requirements and their influence on the parameter estimate have been investigated by Henderson et al [2], yet the application of these models in the clinical setting is difficult and requires a high sampling rate for the arterial input function (AIF). Models using an assumed AIF [1] are more likely to enter the clinical routine since they do not require the identification of arteries or special protocols to meet the temporal requirements for the AIF. One important problem in dynamic contrast-enhanced MRI is the trade off between temporal and spatial resolution [4]. In breast MRI, a high spatial resolution is needed to identify small lesions thus limiting the temporal sampling rate to 5-10 timepoints over a total measurement time of about 5 minutes. It may be questionable whether it is justified to analyze these data without considering the limitations of such measurement. Therefore, this paper investigates the influence of the temporal resolution. This was accomplished by comparing simulated enhancement curves from the tofts with the estimated curves calculated from downsampled data. Moreover, we examine the influence of shifting in analogy to the different bolus arrival times the shift.

**Methods and Materials:** Three simulated datasets with different enhancement characteristics were used as a starting point for the investigation: one curve representing a slow enhancing lesion ( $k = 0.11 \text{ min}^{-1}$ ,  $v_1 = 0.31$ ), one curve representing a tissue with medium permeability ( $k = 0.51 \text{ min}^{-1}$ ,  $v_1 = 0.76$ ) and the third dataset representing tissue with high permeability ( $k = 1.23 \text{ min}^{-1}$ ,  $v_1 = 0.69$ ). These values were derived from the original paper by Tofts [4] as well as the physiological parameters required by the tofts model: plasma amplitudes  $a_1 = 3.99 \text{ kg/l}$ ,  $a_2 = 4.78 \text{ kg/l}$ , plasma exchange rates  $m_1 = 0.144 \text{ min}^{-1}$  and  $m_2 = 0.0111 \text{ min}^{-1}$ , tissue relaxivities  $R_1 = 4.5 \text{ (s}^{-1}\text{mMol)}^{-1}$  and  $R_2 = 5.5 \text{ (s}^{-1}\text{mMol)}^{-1}$ . The protocol simulated was a spoilt gradient echo sequence at 1.5 T with repetition time TR = 50 ms, echo time TE = 6 ms and flip angle  $\alpha = 60^\circ$ . The dose D was set to 0.1 mmol/kg and the arrival time after injection is set to 100 s. Based on these parameter settings the enhancement curves have been simulated with a temporal resolution of 0.3 s for measurement duration of 5 minutes and 10 seconds. The datasets have been downsampled for different temporal resolutions ranging from 5 s up to 1 minute. Additionally, a phase was added to the sampling grid ranging from  $-\pi$  to  $+\pi$  where  $-\pi$  denotes the left border of the sampling interval and  $+\pi$  the right, respectively. The phase was varied with a stepsize of  $1/100 \pi$ . Furthermore, Gaussian noise with  $\sigma = 0.022$ , estimated from a real breast MRI exam, has been added to the downsampled enhancement. Figure 1 shows an example of the modelled, the downsampled and the reconstructed curve for the fast enhancing model settings. The parameters estimated with the phase variation were averaged and the standard deviation has been determined for each different sample width.

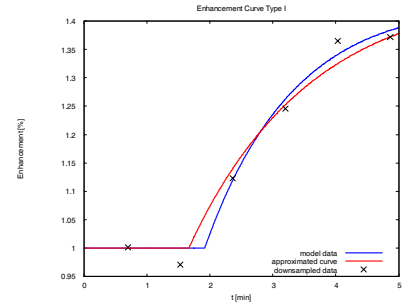


Figure 1: Example for the modelled (blue) and extracted curves (red). The down sampled data is shown as black crosses.

**Results:** Figure 2 shows the results of the simulation for the different model settings. As expected, the standard deviation of optimization results is increasing with decreasing temporal resolution both for  $k_{\text{trans}}$  and  $v_1$ . The absolute variation of  $k$  is increasing with faster enhancement whereas those of  $v_1$  decreases. The maximum error for  $k$  is about  $0.7 \text{ min}^{-1}$  and the one of  $v_1$  is 23%. The highest relative error for  $k$  is 81% and 66% for  $v_1$ , respectively. The relative error for  $k$  increases in the fast enhancing case with increasing sample width ranges from about 4% for a temporal resolution of 5 s to 16% for a temporal resolution of 42 s. For lower temporal resolution, the error is increasing much more strongly up to 81%. In the slow enhancing case, the relative error of  $v_1$  is ranging from 13% for the smallest sampling width to about 66% for the largest one. Remarkable is that  $k$  is underestimated and  $v_1$  is overestimated in the medium enhancing case for sampling widths above 0.6 min.

## Discussion

The results confirm that the application of models is only possible with a sufficient temporal resolution. Protocols used nowadays for breast MRI with a temporal resolution from 0.5 to 1 minute are inapplicable for model simulation since they would result in errors of 16 to 81% for the estimated parameters even under ideal conditions without motion artefacts. Therefore it is either necessary to sacrifice some of the spatial resolution in order to apply pharmacokinetic models like Tofts or to use MR imagers with higher magnetic field strength which allow a faster acquisition or the use of parallel imaging techniques. The results of this study can give a guideline of the required temporal resolution for dynamic contrast enhanced MRI of the breast. Nonetheless, the impact of these results on malignancy estimations has to be evaluated with additional clinical studies on the accuracy requirements for the model parameters. Similar investigations on other models and entities can give similar error estimates and should be undertaken prior to the application of contrast agent models.

## References

- [1] Tofts PS, et al., Magn Reson Med, 33: 564-568 (1995); Brix G, et al., J Comput Assist Tomogr, 15: 621-628 (1991)
- [2] Henderson E, et al., Magn Reson Imag, 16: 1057-1073 (1998)
- [3] Kuhl K, et al., Radiology, 236:789-800
- [4] Tofts PS, et al., J Magn Reson Imaging, 7: 91-101 (1997)

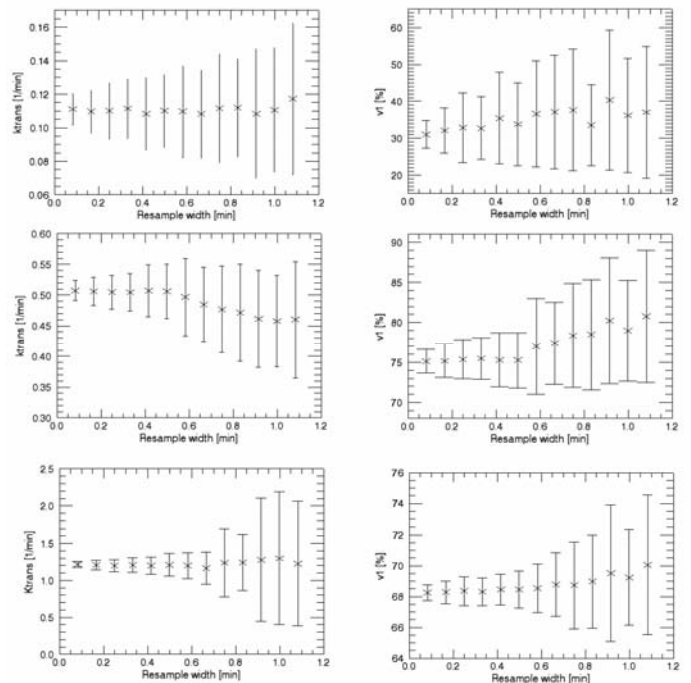


Figure 2: Results of the approximations. Shown are the results for the slow (top), the medium (middle) and fast enhancing (bottom) model settings. All diagrams show the mean and the standard deviations of the approximated parameters.